Sixth International Symposium on Turbulence and Shear Flow Phenomena
Seoul, Korea, 22-24 June 2009

REYNOLDS STRESS MEASUREMENTS IN THE WAKE OF A STACK PARTIALLY IMMERSED IN A TURBULENT BOUNDARY LAYER

Muyiwa S. Adaramola
Division of Environmental Engineering,
University of Saskatchewan
57 Campus Drive, Saskatoon, Saskatchewan, Canada S7N 5A9
muyiwa.adaramola@usask.ca (Alternative email: muyiwa.adaramola@ntnu.no)

Donald J. Bergstrom
Department of Mechanical Engineering,
University of Saskatchewan
57 Campus Drive, Saskatoon, Saskatchewan, Canada S7N 5A9
don.bergstrom@usask.ca

David Sumner
Department of Mechanical Engineering,
University of Saskatchewan
57 Campus Drive, Saskatoon, Saskatchewan, Canada S7N 5A9
david.sumner@usask.ca

ABSTRACT

Some characteristics of the Reynolds stress field in the wake of a stack were experimentally studied in a low-speed wind tunnel using thermal anemometry. The cross-flow Reynolds number was $Re_D = 2.3\times10^4$, and the jet-to-cross-flow velocity ratio was varied from $R = 0$ to 3. The stack was partially immersed in a flat-plate turbulent boundary layer, with a boundary layer thickness-to-stack-height ratio of $\delta/H = 0.5$ at the location of the stack. The spanwise characteristics of the time-averaged streamwise and wall-normal velocities varied along the stack height (z/H) and with the value of R. Likewise, the streamwise and wall-normal turbulence intensities as well as the Reynolds shear stress varied with the stack height z/H and were strongly influenced by the value of R. The behaviour of the shear correlation coefficient indicated that there is more turbulent mixing within the vicinity of the free end of the stack than at mid-height.

INTRODUCTION

The complex flow field associated with a stack is encountered in many engineering applications, especially in the area of pollution dispersion. The mixing and dispersion of the jet issuing from a stack depend on the ambient conditions, the jet exit characteristics, and the geometry of the stack. The simplest stack geometry can be represented by a uniform finite circular cylinder mounted normal to a ground plane. Due to the influence of the free end and the boundary layer on the ground plane, there are marked changes in the near-wake flow structure along the cylinder height. These changes are strongly influenced by the cylinder's aspect ratio, AR (= H/D, where H and D are the height and diameter of the cylinder, respectively). Two pairs of counter-rotating streamwise vortex structures have been identified within the wake of the finite circular cylinder (Sumner *et al*. 2004). The first pair, called the tip vortex structures, is formed very close to the free end and is associated with a downward directed velocity along the wake centreline known as "downwash", while the second pair, called the base vortex structures, is found close to the ground plane. Kármán vortex shedding from the finite circular cylinder is influenced by the tip vortices (Sumner *et al*. 2004).

Compared with a finite circular cylinder, the presence of the jet flow issuing from the stack gives rise to an even more complicated flow structure, both around the stack and in its wake. For a non-buoyant jet, the extent of this complexity depends on the jet-to-cross-flow velocity ratio, R (= U_e/U_∞, where U_e and U_∞ are the mean jet exit velocity and the freestream velocity, respectively). The flow regimes in the stack wake have been classified differently by various researchers. For example, three distinct flow regimes have been identified for R varying between 0 and 3: the downwash flow regime for $R < 0.7$, the crosswind-dominated flow regime for $0.7 \leq R < 1.5$, and the jet-dominated flow regime for $R \geq 1.5$ (Adaramola *et al*. 2007). Each flow regime has distinct flow structures evident within the turbulence and time-averaged velocity fields (Adaramola *et al*. 2007 and Adaramola *et al*. 2007b). Various zones can also be identified within the jet itself, depending on the value of R and the corresponding flow regime (Mahjoub Saïd *et al*. 2005). Recently, Adaramola *et al.* (2007a) identified up to three pairs of streamwise vortex structures within the stack wake (Fig. 1), depending on the value of R. These vortex structures influence the turbulence characteristics within the wake of the stack. In the downwash flow regime (Fig. 1(a)),

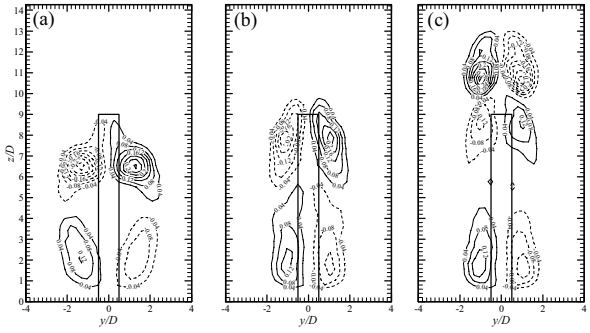

Figure 1: Mean streamwise vorticity field (iso-vorticity contours of $\omega_x^*=\omega_x D/U_\infty$) downstream of the stack at x/D = 6, from Adaramola et al. (2007a), for (a) R = 0.5; (b) R = 1; and (c) R = 2.5. Solid lines represent positive (CCW) vorticity; dashed contour lines represent negative (CW) vorticity. Minimum vorticity contour of $\omega_x^*= \pm 0.04$, and contour increment of $\Delta\omega_x^*= 0.04$.

two pairs of counter-rotating streamwise vortex structures, each of opposite sign, are found. The characteristics of these structures are similar to those of the finite circular cylinder (Sumner *et al*. 2004), with the tip vortex pair located closer to the free end of the stack and the base vortex pair located within the flat-plate boundary layer on the ground plane. The same vortex pairs are found in the crosswind-dominated flow regime (Fig. 1(b)), but the tip vortex pair extends above the free end of the stack. In case of the jet-dominated flow regime (Fig. 1(c)), a third pair of streamwise vortices, referred to as the jet-wake vortex pair, appears in the jet wake region above the free end of the stack. The jet-wake vortex structures are associated with the jet rise and a strong upwash velocity on the jet wake centreline.

Notwithstanding the practical significance of this flow, the experimental data base is in many ways incomplete. For example, there is limited information about the characteristics of the Reynolds stress in the wake of a stack. This information is important for any validation of computational studies, and also supports a better understanding of the overall flow structure. Adaramola *et al.* (2007b) reported some of the effects of R on the turbulence statistics within the wake of a stack but suggested that further study of this flow should also include measurements in the x-y and x-z planes. The present study reports on some of these measurements.

EXPERIMENTAL APPROACH

The present experiments were conducted in a low-speed, closed-return wind tunnel with a test section of 0.91 m (height) × 1.13 m (width) × 1.96 m (length). The streamwise freestream turbulence intensity was less than 0.6% and the velocity non-uniformity outside the test section wall boundary layers was less than 0.5%. The test section floor was fitted with a ground plane. A roughness strip located about 200 mm from the leading edge of the ground plane was used to enhance the development of a turbulent boundary layer. At the location of the stack (with the stack removed), the boundary layer provided a thickness-to-height ratio of $\delta/H \approx 0.5$, and the Reynolds number based on momentum thickness, θ, was $\mathrm{Re}_\theta = 8\times10^3$. The experimental

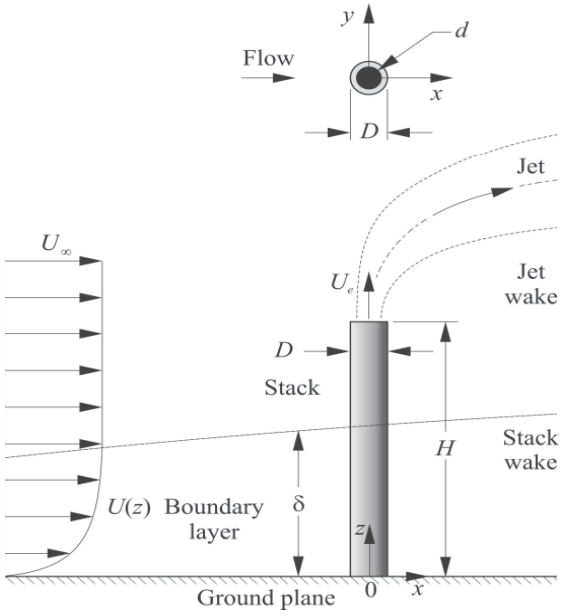

Figure 2: Schematic of a cylindrical stack mounted normal to a ground plane and partially immersed in a plane boundary layer.

set-up for the study is shown schematically in Fig. 2, and was similar to that adopted by Adaramola *et al*. (2007).

Experimental Apparatus

A cylindrical stack of H = 171.5 mm, D = 19.1 mm, d/D = 0.67 (where d is the internal diameter), and AR = 9, was used in the present study. The stack was located 700 mm downstream of the roughness strip on the ground plane. The experiments were conducted at a single stack Reynolds number (based on D and U_∞) of $\mathrm{Re}_D = 2.3\times10^4$. The exhaust velocity of the non-buoyant stack jet was varied with two MKS 1559A-200L mass flow controllers arranged in parallel. The jet-to-cross-flow velocity ratio was varied from R = 0 (no jet exiting the stack) to R = 3. The jet Reynolds number, Re_d (based on d and U_e) ranged from 7.6×10^3 to 4.7×10^4.

Measurement Instrumentation

The wind tunnel data were acquired by a computer with a 1.8-GHz Intel Pentium 4 processor, a National Instruments PCI-6031E 16-bit data acquisition board, and LabVIEW software. The freestream conditions were obtained with a Pitot-static probe (United Sensor, 3.2-mm diameter), Datametrics Barocell absolute and differential pressure transducers, and an Analog Devices AD590 integrated circuit temperature transducer.

Turbulent velocity measurements were made with a TSI model 1243-20 boundary layer X-probe and a TSI IFA-100 constant-temperature anemometer. Time-averaged velocity measurements were also made with a seven-hole pressure probe. Each probe was manoeuvred to the measuring points using the wind tunnel's three-axis computer-controlled traversing system. At each measurement point, 100,000 instantaneous velocity data per channel were acquired at a sampling rate of 10 kHz per channel after low-pass filtering at 5 kHz. The uncertainties

in the streamwise and wall-normal fluctuating velocity components were estimated to be ±4% and ±7%, respectively, while the uncertainty in the Reynolds shear stress was estimated to be ± 9%. The measurement plane extended to z/D = 14 in the wall-normal direction. The X-probe was oriented to measure the streamwise, u, and wall-normal, w, velocity components, while the seven-hole probe measured all three components of the time-averaged velocity field (u,v,w). Measurements were made in the central region of the y-z plane at x/D = 10 (where x is the streamwise distance from the stack).

RESULTS AND DISCUSSION

In this paper, measurements for R = 0.5 (downwash flow regime), R = 1 (crosswind-dominated flow regime) and R = 2.5 (jet-dominated flow regime), which represent the three distinct flow regimes identified by Adaramola *et al.* (2007), are presented and discussed. In addition, the data for R = 0, which represent the finite circular cylinder case, are also included. Due to space constraints, only the results at vertical positions of z/H = 0.5 and 0.75 are presented in this paper.

Time-Averaged Velocity Profiles

The time-averaged streamwise velocity profiles (u/U_∞) at x/D = 10 and at two different vertical locations along the stack height are shown in Fig. 3. At z/H = 0.5 (Fig. 3(a)), a strong streamwise velocity defect (with similar profiles) was observed for all three flow regimes, although the peak of the defect reduces as the regime changes from downwash flow to jet-dominated flow. At z/H = 0.75 (Fig. 3 (b)), two peaks are observed for the downwash flow regime while a single peak is observed for the crosswind-dominated flow regime and the jet-dominated flow regime. The appearance of two peaks in the profile for the downwash flow regime may be caused by the effect of the downwash flow from the stack free end (Okamoto and Sunabashiri, 1992). For this flow regime, the streamwise velocity decreases gradually from the wake centreline to reach a minimum value at about ±1.5D and then increases gradually to the freestream value at about ±3D from the wake centreline. The single peak in the defect velocity observed for the crosswind-dominated flow regime and the jet-dominated flow regime shows the influence and the presence of the strong jet flow which tends to increase the effective aspect ratio of the stack (Adaramola et al., 2007). For these flow regimes, the velocity increases gradually from the wake centreline to attain the freestream value at about ± 3D on either side of the wake centreline. In contrast, the profile for the finite cylinder (with no jet flow) is nearly uniform (u/U_∞ = 1) which indicates that this location is outside the velocity defect (wake) region.

The time-averaged wall-normal velocity profiles (w/U_∞) at x/D = 10 and at two different vertical locations along the stack height are shown in Fig. 4. At z/H = 0.5 (Fig. 4(a)), the profiles for the crosswind-dominated flow and jet-dominated flow regimes (R = 1 and 2.5, respectively) indicate the presence of upwash flow ($+w/U_\infty$) within the vicinity of the wake centreline at this region of the stack. In contrast, for the downwash flow regime (R = 0.5), the profile

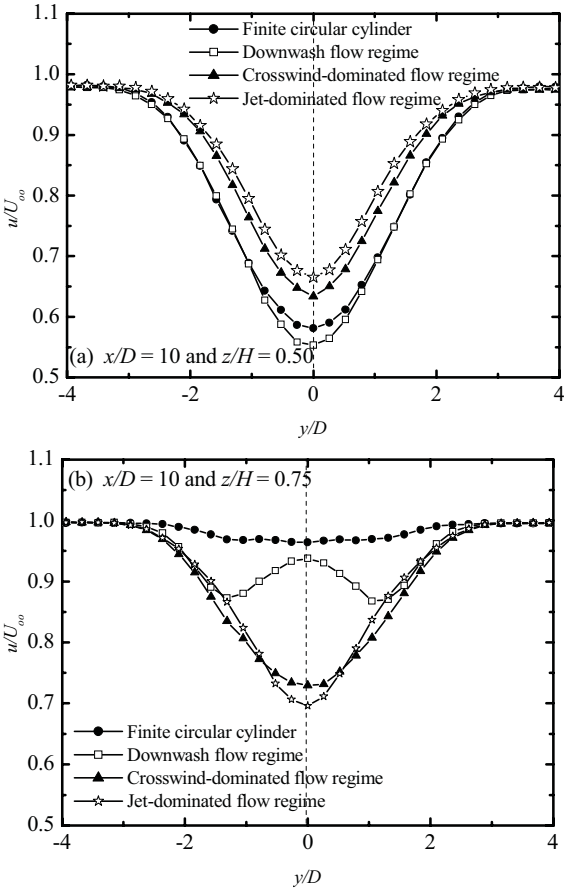

Figure 3: The time-averaged streamwise velocity (u/U_∞) profiles at x/D = 10: (a) z/H = 0.5 and (b) z/H = 0.75.

is nearly uniform and equal to zero. For the finite cylinder (R = 0), the presence of downwash flow ($-w/U_\infty$) is observed within the vicinity of the wake centreline. The reason for the observed profile in the case of the downwash flow regime is that the jet flow is too weak to penetrate the crossflow but strong enough to prevent the downwash flow from moving into this region of the stack. At z/H = 0.75 (Fig. 4(b)), downwash flow is present for all the flow regimes within the vicinity of the wake centreline but its absolute value depends on the flow regime. As expected, the strength of the downwash flow at this location is stronger for the downwash flow regime than for the crosswind-dominated and jet-dominated flow regimes. This is related to the strength of the tip vortex structures which decreases as the flow regime changes from the downwash flow to jet-dominated flow regime (see Fig. 1). Also, the presence of the weak jet flow in the case of the downwash flow regime (R = 0.5) increases the amount of jet flow in the wake and this explains the reason for the stronger downwash flow for this regime than for the finite cylinder (R = 0). In addition, the stronger downwash flow observed in the downwash flow regime profile when compared with the finite cylinder profile is related to the tip vortex structures which are stronger at z/H = 0.75 for R = 0.5 than R = 0. Between y/D = ±2 and ±3, a small region of upwash flow is observed for all three flow regimes.

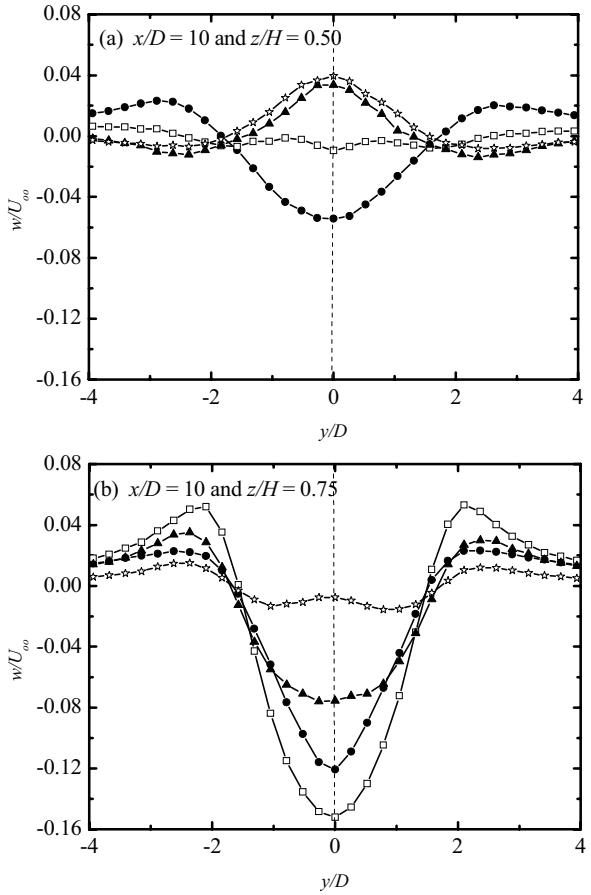

Figure 4: The time-averaged wall-normal velocity (w/U_∞) profiles at x/D = 10: (a) z/H = 0.5 and (b) z/H = 0.75 (symbols as defined in Fig. 3).

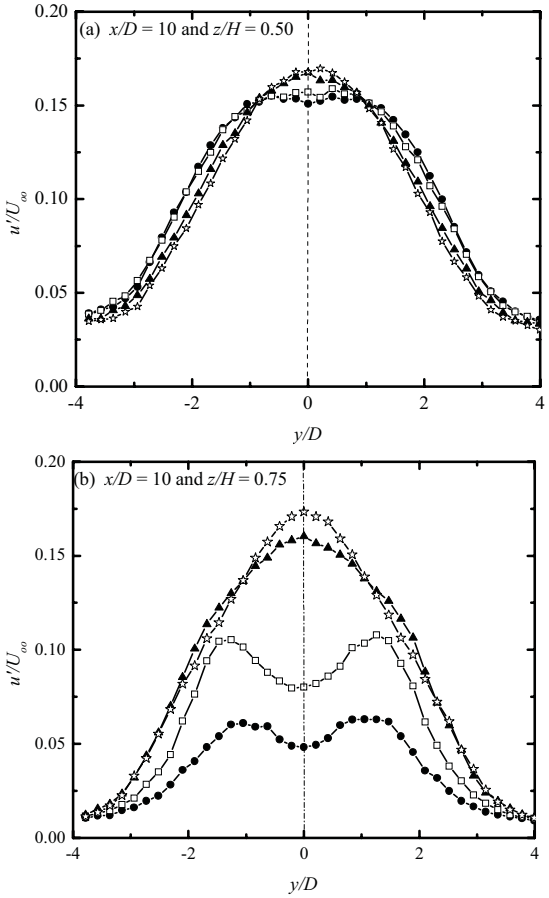

Figure 5: The streamwise turbulence intensity profiles at x/D = 10: (a) z/H = 0.5 and (b) z/H = 0.75 (symbols as defined in Fig. 3).

Turbulence Intensity

The streamwise turbulence intensity profiles (u'/U_∞) at x/D = 10 and at two different vertical locations along the stack height are shown in Fig. 5. As would be expected, the turbulence intensity profiles are symmetrical about the wake centreline (y/D = 0) at all locations. At z/H = 0.5 (Fig. 5(a)), a small double peak is observed for the finite cylinder (R = 0). This is similar to the results of Okamoto and Sunabashiri (1992) for AR = 7 at x/D = 10 and Afgan et al. (2007) for AR = 6 at x/D = 5. Similar characteristics for the finite circular cylinder were also reported by Adaramola et al. (2006) for a cylinder with AR ≥ 5. The profile for the downwash flow (R = 0.5) is similar to that of the finite circular cylinder. However, in the case of the crosswind-dominated and jet-dominated flow regimes (R = 1 and 2.5, respectively), only a single peak is observed. At z/H = 0.75 (Fig. 5(b)), a twin-peak profile is observed for the finite cylinder and the downwash flow regime (R = 0 and 0.5, respectively). The turbulence intensity increases gradually from the wake centreline to reach a maximum value at about ±1D and then decreases gradually to the freestream value at about ±4D from the wake centreline. The two peaks observed may be related to the downwash flow from the stack free end and may also be related to the separated shear layers from the stack surface. Wang *et al.* (2006) also observed two peaks in the streamwise turbulence intensity for a finite-length square cylinder of AR = 5 at z/H = 0.8 and x/D = 6. In contrast, a single peak is observed for the crosswind-dominated and jet-dominated flow regimes. The turbulence intensity at the wake centreline increases with the value of R. The strong turbulence is likely due to the enhanced shear associated with the tip vortex pair which extends above the stack free end for the crosswind-dominated flow regime and the jet-wake vortex pair for the jet-dominated flow regime.

The wall-normal turbulence intensity profiles (w'/U_∞) at x/D = 10 and at two different vertical locations along the stack height are shown in Fig. 6. At z/H = 0.5 (Fig. 6(a)), two peaks are observed for the downwash and crosswind-dominated flow regimes, while a broad single peak is observed for the jet-dominated flow regime. At z/H = 0.75 (Fig. 6(b)), similar to the streamwise turbulence intensity profile (Fig. 5(b)), a twin-peak distribution is observed for the finite cylinder and the downwash flow regime, which is also consistent with previous measurements for a finite cylinder of AR = 9 (Adaramola et al., 2006). A single peak is, however, observed for the crosswind-dominated and jet-dominated flow regimes. In contrast to this study, Wang *et al.* (2006) observed only one peak in the wall-normal turbulence intensity profile for a square cylinder of AR = 5 at z/H = 0.8 and x/D = 6. Generally, the wall-normal turbulence intensity at the wake centreline increases with R. Meanwhile, irrespective of the location, there is a strong similarity between the wall-normal and streamwise

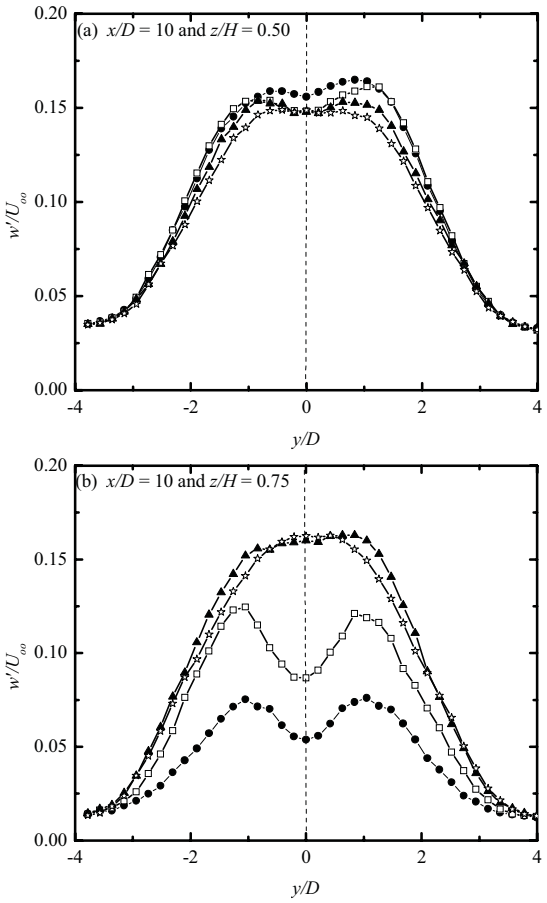

Figure 6: The wall-normal turbulence intensity profiles at x/D = 10: (a) z/H = 0.5 and (b) z/H = 0.75 (symbols as defined in Fig. 3).

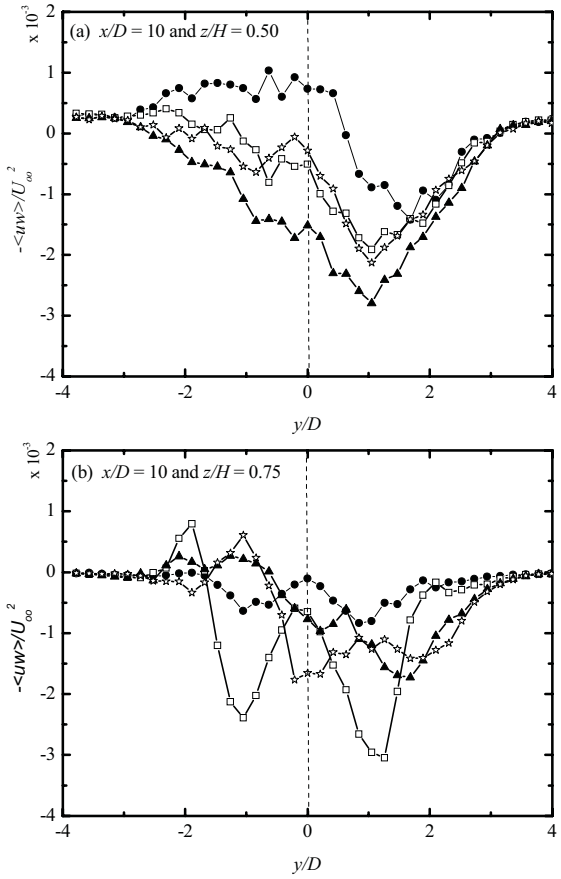

Figure 7: The Reynolds shear stress profiles at x/D = 10: (a) z/H = 0.5 and (b) z/H = 0.75 (symbols as defined in Fig. 3).

turbulence intensity profiles for each flow regimes. This similarity is evident in both the shape and approximate magnitude of the profiles. The anisotropy parameter, $\eta = w'^2/u'^2$ provides information about the deviation of the flow from an isotropic state (η = 1). The value of η (not shown) was found to depend on the flow regime and vary with the location along the stack height as well as the spanwise location. For example, along the wake centreline the values of η ranges between about 0.9 (for the jet-dominated flow regime) and about 1.2 (for downwash flow regime) at z/H = 0.75.

Reynolds Shear Stress

The Reynolds shear stress profiles ($-\langle uw\rangle/U_\infty^2$) at x/D = 10 and at two different vertical locations along the stack height are shown in Fig. 7. At z/H = 0.5 (Fig. 7(a)), the finite cylinder data exhibit a distinct peak on the positive side of the stack and a broad-band peak on the negative side. The downwash flow regime (R = 0.5) and the crosswind-dominated flow regime (R = 1) have similar profiles that decrease from about y/D = -3 and attain a minimum value at about y/D = 1, then increase again to attain the freestream value at about y/D = 3. However, at each spanwise location more negative values are obtained for the crosswind-dominated flow regime compared with the downwash flow regime. For the jet-dominated flow regime, two local minima are observed on either side of the stack. At z/H = 0.75 (Fig. 7(b)), the effect of the flow regime on the shear stress is more dramatic and complex when compared with the profiles at z/H = 0.5. This complexity is related to the tip vortex structures near the free end of the stack (see Fig. 1). The strong peaks observed for the downwash flow regime may be related to the stronger vortex structure for this regime in this region of the stack when compared with the other flow regimes.

Comparing the data in Fig. 7 with the data in Fig. 5 and 6, as expected, the shear stress values are seen to be smaller in magnitude than both the streamwise and wall-normal turbulence intensities. In order to assess the degree of organization in the turbulent motions, the shear correlation coefficient R_{uw} (= $\langle uw\rangle/u'w'$) profiles are presented in Fig. 8. The shear correlation can be interpreted as a measure of the efficiency of turbulent mixing and its value lies between -1 and 1 (Jovic, 1996). A positive correlation implies that when u is positive, v is likely to also be positive and vice versa. A negative correlation implies that it is more likely that the velocity fluctuations have different signs. At z/H = 0.5 (Fig. 8a), within the vicinity of the wake centreline ($-3 < y/D < 3$), there is gradual reduction in R_{uw} from the left to right side of the stack. Although the observed trend is similar for all of the flow regimes, their values are slightly different and reduce as the flow changes from the downwash to the jet-dominated flow regime. At z/H = 0.75 (Fig. 8(b)), the profiles for the crosswind-dominated and jet-dominated flow regimes are similar. Unlike the

profiles at z/H = 0.5 (Fig. 8(a)), the profiles for the downwash flow regime and the finite cylinder are distinct from those of crosswind-dominated and jet-dominated flow regimes. This is related to the strength of the tip vortex structures, which are weaker for the crosswind-dominated and jet-dominated flow regimes when compared with downwash flow regime. For these two flow regimes, the correlation coefficient varies dramatically across the flow, which is evidence of rapid changes in the local flow structure.

CONCLUSIONS

In this study, the effect of the jet-to-cross-flow velocity ratio, R, on the characteristics of the Reynolds stresses within the wake of a short stack was investigated experimentally using two-component thermal anemometry. The results demonstrate the strong influence of the jet velocity (or flow regime) on the streamwise and wall-normal velocity components as well as on the Reynolds stresses. In addition, the behaviour of these parameters was strongly influenced by the spanwise location along the stack height. At the mid-height of the stack, the effect of the flow regime on the time-averaged velocity and Reynolds stresses was not as pronounced as for a section near the free end (z/H = 0.75). The behaviour of the shear correlation coefficient indicated that there is more energetic turbulent mixing within the vicinity of the free end of the stack than at mid-height.

The measurements presented in this study demonstrate the complexity of the flow structures within the combined wake of a stack and jet flow. Further study of the combined wake region, with measurements in other planes and of the remaining velocity and Reynolds stress components, would be beneficial. For example, a more complete data base would enable an assessment of the production terms in the Reynolds stress transport equations and thereby facilitate an improved understanding of the effect of the complex velocity gradients on the turbulence structure and hence mixing in the wake.

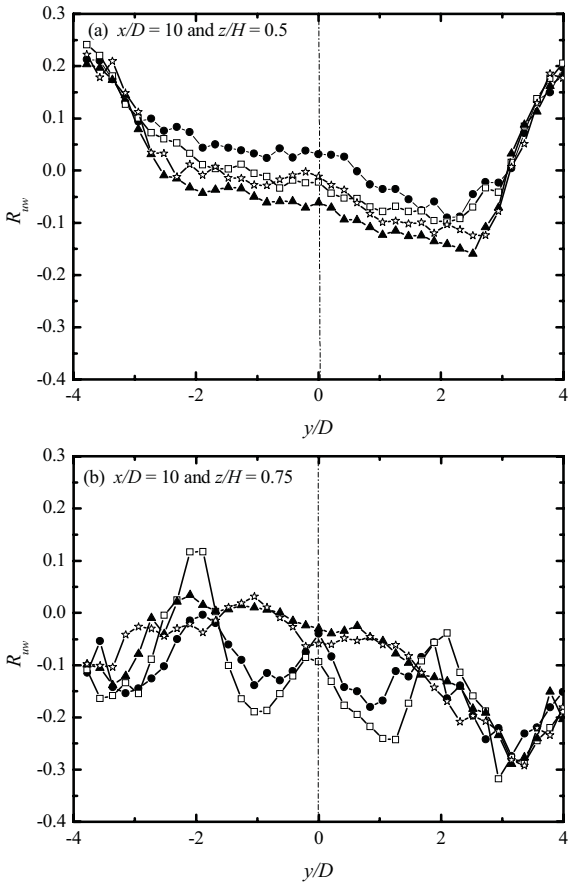

Figure 8: The shear correlation coefficient profiles at x/D = 10: (a) z/H = 0.5 and (b) z/H = 0.75 (symbols as defined in Fig. 3).

REFERENCES

Adaramola, M.S., Akinlade, O.J., Sumner, D., Bergstrom, D.J., Schenstead, A.J., 2006. Turbulent wake of a finite circular cylinder of small aspect ratio. *Journal Fluids and Structures* **22**, 919-928.

Adaramola M.S., Bergstrom D.J., Sumner D., 2007a. Effect of velocity ratio on the vortex structures within the wake of a stack. *Proceedings of the IUTAM Symposium on Unsteady Separated Flows and their Control,* Corfu, Greece, June 18-22, 2007.

Adaramola M.S., Bergstrom D.J., Sumner D., 2007b. The turbulent statistics in the wake of a short stack. *Proceedings of the 5th Int. Symp. on Turbulence and Shear Flow Phenomena* (TSFP-5), Munich, Germany, August 27-29, 2007, 643-648.

Adaramola, M.S., Sumner, D., Bergstrom, D.J., 2007. Turbulent wake and vortex shedding for a partially immersed in a turbulent boundary layer. *Journal of Fluids and Structures* **23**, 1189-1206.

Afgan, I., Moulinec, C., Prosser, R., Laurence, D., 2007. Large eddy simulation of turbulent flow for wall mounted cantilever cylinders of aspect ratio 6 and 10. *International Journal of Heat and Fluid Flow* **28**, 561–574.

Huang, R.F., Hsieh, R.H., 2003. Sectional flow structures in near wake of elevated jet in a crossflow. *AIAA Journal* 41, 1490-1499.

Jovic, S., 1996. An experimental study of a separated/Reattached flow behind a backward facing step. NASA Technical Memorandum 110384.

Mahjoub Saïd, N., Mhiri, H., Le Palec, G., Bournot, P., 2005. Experimental and numerical analysis of pollutant. dispersion from a chimney. *Atmospheric Environment* 39, 1727-1738.

Okamoto, S., Sunabashiri, Y., 1992. Vortex shedding from a circular cylinder of finite length placed on a ground plane, *ASME Journal of Fluids Engineering* 144, 512-521.

Sumner, D., Heseltine, J.L., and Dansereau, O.J.P., 2004. Wake structure of a finite circular cylinder of small aspect ratio. *Experiments in Fluids* 37, 720-730.

Tanaka, S., Murata, S., 1999. An investigation of the wake structure and aerodynamic characteristics of a finite circular cylinder. *JSME International Journal Series B: Fluids and Thermal Engineering* 42, 178-187.

Wang, H.F., Zhou, Y., Chan, C.K., Lam, K.S., 2006. Effect of initial conditions on interaction between a boundary layer and a wall-mounted finite-length-cylinder wake. *Physics of Fluids* 18, 065106.